Digital Carrier Frequency Estimation For Multilevel CPM Signals

A. N. D'Andrea, A. Ginesi and U. Mengali

University of Pisa
Department of Information Engineering
Via Diotisalvi 2, 56126, Pisa, Italy

Abstract – **This paper analyzes a feedforward synchronization scheme for carrier frequency recovery in continuous phase modulation. The algorithm is non-data-aided and non-clock-aided and can be implemented in digital form. It operates with general multilevel partial response signaling. Because of its feedforward structure, its estimation time is independent of the frequency offset. Its estimation range is large, on the order of the symbol rate. Performance is investigated theoretically and is checked by simulation.**

1. Introduction

Carrier frequency compensation is needed in digital receivers to cope with oscillator instabilities and/or Doppler effects. Compensation is carried out by first deriving an estimate $\hat{\nu}$ of the carrier frequency shift from its nominal value, and then counter-rotating the received signal samples by a steadily advancing phase $\theta(k)=2\pi\hat{\nu}kT_s$, ($k$=..-1, 0, 1..), where T_s is the sampling period.

A few frequency estimators [1]-[3] are available for continuous phase modulation (CPM). Reference [1] investigates a data-aided feedforward algorithm for Gaussian MSK. Its performance is remarkably close to the modified Cramer-Rao bound but its operation range is limited to a few percents of the bit rate. This tends to disqualify it from general use as an acquisition aid. The algorithm proposed in [2] has still a feedforward structure, but is non-data-aided and is suitable for MSK modulation. Although its performance does not attain the modified Cramer-Rao bound, it can manage much larger frequency offsets, say up to 25% of the bit rate. Finally, a non-data-aided and non-clock-aided feedback structure is proposed in [3] for MSK-type signals. Its tracking performance is worse than in the prior schemes but its estimation range is larger, on the order of the bit rate.

All of the above methods deal with *binary* modulations. In this paper we analyze a non-data-aided and non-clock-aided feedforward scheme operating with general *M-ary* modulations. This scheme has a *delay-and-multiply* structure like that proposed in [4] for PSK/QAM signals. Its estimation range is on the order of the symbol rate, i.e., approximately as in [3]. In comparison with [3], however, it can deal with multilevel signaling and provides better frequency estimates. Also, its estimation time is fixed, i.e., independent of the actual frequency offset.

2. Signal Model

The complex envelope of the received waveform is the sum of signal plus noise:

$$r(t)=s(t)+w(t). \tag{1}$$

The noise w(t) is modelled as a complex-valued white Gaussian process with power spectral density $2N_0$. The signal has the form

$$s(t)=\sqrt{\frac{2E_s}{T}}\,e^{j[2\pi\nu t+\theta+\psi(t)]}, \tag{2}$$

where E_s is the signal energy per symbol, T is the symbol period, ν is the unknown carrier frequency offset, θ is a constant which accounts for the channel phase shift, and $\psi(t)$ represents the *information bearing function*

$$\psi(t)=2\pi h\sum_i \alpha_i q(t-iT). \tag{3}$$

The parameter h in (3) is the modulation index, α_i are independent data symbols taken from the alphabet $\{\pm1,\pm3...\pm(M\text{-}1)\}$ and $q(t)$ is the so-called *phase pulse* of the modulator. This function is related to the *frequency pulse* $g(t)$ by

$$q(t)=\int_{-\infty}^{t} g(\tau)d\tau. \tag{4}$$

The latter is time limited to the interval $(0, LT)$ and is scaled so that the integral in (4) equals 1/2 for $t\geq LT$.

In numerical examples illustrated later we consider two forms of $g(t)$: (1) rectangular of length LT (LREC); (2) Gaussian MSK (GMSK) with a shaping filter bandwidth B=0.25/T.

3. Frequency Estimation Algorithm

The block diagram of the frequency estimator is illustrated in Fig. 1.

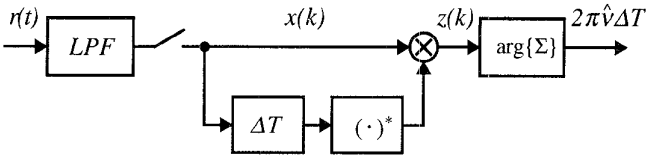

Fig. 1. Block diagram of the frequency estimator.

The incoming waveform is first passed through a low-pass filter (LPF) to eliminate as much noise as possible. To simplify the discussion we assume an LPF with an ideal brick-wall transfer function. This shape is not exactly met in practice but the ensuing arguments are easily adapted to any realistic filter. We also assume that the filter bandwidth B_{LPF} is wide enough to pass the signal undistorted even when the frequency offset is at its maximum. With many CPM formats the signal spectrum extends over a range of about $\pm1/T$ around ν. Thus, if we allow ν values up to about $\pm1/T$, B_{LPF} should be somewhere between $2/T$ and $3/T$. For simplicity, in this study we consider only two cases

$$B_{LPF}=\begin{cases}2/T\\3/T.\end{cases} \tag{5}$$

The filter output $x(t)=s(t)+n(t)$ is sampled at $t=kT_s+t_0$ (k=..-1,0,1..), where $t_0\in(0,T_s)$ is an arbitrary constant and

0-7803-2486-2/95 $4.00 © 1995 IEEE

$1/T_s=2B_{LPF}$. The samples $x(k)=x(kT_s+t_0)$ contain all the information about $x(t)$ and have independent noise components (because of the shape of the LPF transfer function). Note that, as a consequence of (5), the sampling rate is a multiple of the symbol rate, i.e., $1/T_s=N/T$, with N=4 or N=6, depending on the value of B_{LPF}.

Next, the following products are formed

$$z(k)=x(k)x^*(k-D), \tag{6}$$

where the asterisk denotes complex conjugate, and the integer D corresponds to the delay $\Delta T=DT_s$. For the moment we ignore the role of this delay and we concentrate on the statistics of $z(k)$. As we shall see, they suggest a method to estimate the frequency offset.

Collecting (2) and (6) results in

$$\begin{aligned} z(k) = \frac{2E_s}{T}\, e^{j2\pi\nu\Delta T} e^{j[\psi(k)-\psi(k-D)]} + n(k)n^*(k-D) \\ + n(k)s^*(k-D) + n^*(k-D)s(k). \end{aligned} \tag{7}$$

Hence, taking the expectation over data and noise, gives

$$E\{z(k)\} = \frac{2E_s}{T} A(k)\, e^{j2\pi\nu\Delta T}, \tag{8}$$

where $A(k)$ is short for $A(kT_s+t_0)$ and $A(t)$ is the expectation of $\exp\{j[\psi(t)-\psi(t-\Delta T)]\}$ over the data symbols. An explicit expression for this function is found to be

$$A(t) = \prod_i \left[\frac{1}{M} \times \frac{\sin[2\pi hMa(t-iT)]}{\sin[2\pi ha(t-iT)]}\right], \tag{9}$$

with $a(t)=q(t)-q(t-\Delta T)$. From this equation it is seen that $A(t)$ is a real-valued and periodic function of period T. As such, it needs to be computed on only one symbol interval, say $(0,T)$, since all intervals are identical. Furthermore, it can be shown that most of the factors in (9) are unity for $t\in(0,T)$ and, in fact, the only non-unity factors are those with the index in the range $-[L+\mathrm{int}(\Delta T/T)]\le i\le 0$, where $\mathrm{int}(\Delta T/T)$ means "largest integer not exceeding $\Delta T/T$".

Figure 2 illustrates the shape of $A(t)$ for MSK and a few values of ΔT. Figure 3 compares M=2 with M=4 for 1REC and h=1/2.

As $A(t)$ is periodic of period T and the sampling period T_s equals T/N, it follows that $A(k)$ is periodic of period N. Then, summing (8) for k varying from 1 to a multiple of N, say $N\times L_0$, yields

$$E\left\{\sum_{k=1}^{NL_0} z(k)\right\} = \frac{2E_s}{T} NL_0 \overline{A}\, e^{j2\pi\nu\Delta T}, \tag{10}$$

with

$$\overline{A} = \frac{1}{N}\sum_{k=0}^{N-1} A(k). \tag{11}$$

Now, assuming $\overline{A}>0$, it follows from (10) that

$$\nu = \frac{1}{2\pi\Delta T} \arg E\left\{\sum_{k=1}^{NL_0} z(k)\right\}. \tag{12}$$

(When $\overline{A}$ is negative, the sign of the right-hand side of (12) must be changed). From this equation it appears that, if the expectation $E\{\Sigma\}$ were known, the frequency offset could be computed exactly. In practice $E\{\Sigma\}$ is not known but an estimate of ν may still be obtained by replacing $E\{\Sigma\}$ with Σ. This results in the following frequency estimator

$$\hat{\nu} = \frac{1}{2\pi\Delta T} \arg\left\{\sum_{k=1}^{NL_0} z(k)\right\}, \tag{13}$$

whose performance is analized in the next section.

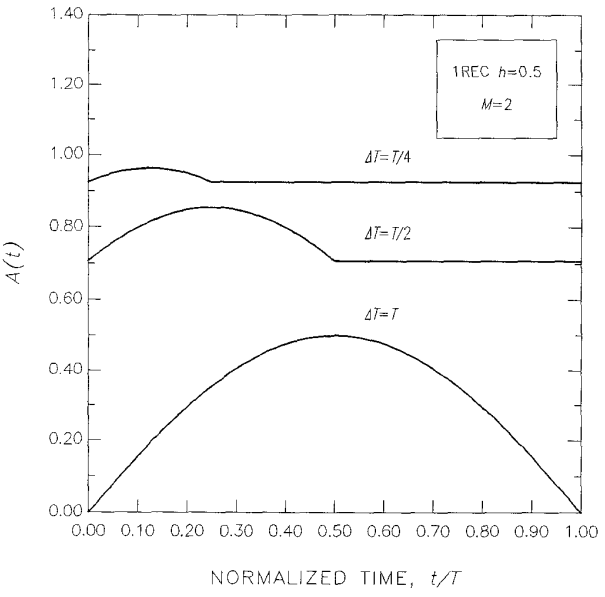

Fig. 2. Shape of $A(t)$ with MSK.

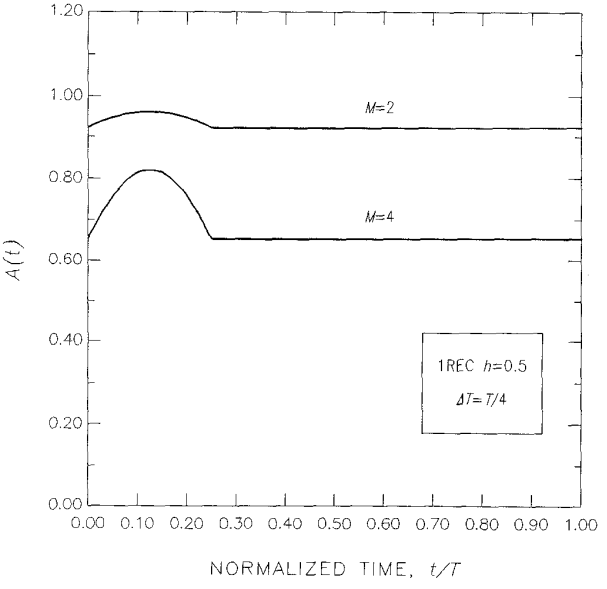

Fig. 3. Shape of $A(t)$ with 1REC and M=2 or M=4.

It is worth noticing that, as the arg{.} function varies between $\pm\pi$, the estimate $\hat{\nu}$ varies between $\pm 1/2\Delta T$. As we are interested in an estimation range of 50% to 100% of the symbol rate, ΔT must be less than T. But, how much less than that? This issue is deferred to Section 5 where simulation results are presented.

4. Analysis

First- and second-order moments of $\hat{\nu}$ are now investigated.

Mean value. An exact derivation of $E\{\hat{\nu}\}$ is difficult because the estimator is nonlinear. We make an approximation that amounts to linearizing the function $\arg\{\cdot\}$ around some operating point. More specifically, call X the sum in (13)

$$X = \sum_{k=1}^{NL_0} z(k), \tag{14}$$

and $\overline{X}$ its expectation. When SNR is high and/or the parameter L_0 is large enough, X is a random variable undergoing small fluctuations around $\overline{X}$. Thus, letting

$$\delta = \frac{X - \overline{X}}{\overline{X}}, \tag{15}$$

we expect that real and imaginary components of δ, say δ_R and δ_I, are small as compared with unity. Note that δ_R and δ_I have zero mean. On the other hand, from (15) it is easily found

$$\arg\{X\} = \left[\arg\left\{\overline{X}\right\} + \arg\left\{1 + \delta_R + j\delta_I\right\}\right]_{-\pi}^{+\pi}, \tag{16}$$

where $[\bullet]_{-\pi}^{+\pi}$ means that the quantity in brackets must be reduced to the interval $\pm\pi$. Hence, making the approximation $\arg\{1+\delta_R+j\delta_I\} \cong \delta_I$ and collecting (13)-(16) yields

$$\hat{\nu} \cong \frac{1}{2\pi\Delta T}\left[2\pi\nu\Delta T + \delta_I\right]_{-\pi}^{+\pi} \tag{17}$$

From this equation it is seen that, when ν is *not too close* to $\pm 1/2\Delta T$, the quantity $2\pi\nu\Delta T+\delta_I$ falls in the interval $\pm\pi$ and (17) reduces to

$$\hat{\nu} \cong \nu + \frac{\delta_I}{2\pi\Delta T}. \tag{18}$$

Under these conditions the expected value of $\hat{\nu}$ coincides with ν. In conclusion, the estimator is unbiased as long as ν is at some distance from the boundaries $\pm 1/2\Delta T$.

What happens when ν gets close to the boundaries? To be specific, suppose that ν is slightly less than $1/2\Delta T$. Then, depending on the value of δ_I, the sum $2\pi\nu\Delta T+\delta_I$ in (17) is either less or greater than π. In the former case (17) gives $\hat{\nu} \cong 1/2\Delta T$ while, in the latter, $\hat{\nu} \cong -1/2\Delta T$. So, the estimate will be close to zero, on average. In conclusion, the expected value of $\hat{\nu}$ approaches zero as ν approaches $\pm 1/2\Delta T$.

Error variance. Assuming that (18) is valid, the estimation error is $\delta_I/2\pi\Delta T$. Computing the variance of this random variable is a tedious task that will not be pursued here due to space limitations. Only the final results are provided. For convenience, errors are normalized to the symbol rate so that their mean square value is

$$\sigma^2 = \left[\frac{T}{2\pi\Delta T}\right]^2 E\left\{\delta_I^2\right\}. \tag{19}$$

It is found that σ^2 is the sum of three terms

$$\sigma^2 = \sigma_{SS}^2 + \sigma_{SN}^2 + \sigma_{NN}^2, \tag{20}$$

corresponding to interactions Signal×Signal, Signal×Noise and Noise×Noise arising in the estimation process. For L_0>>1 these terms are given by

$$\sigma_{NN}^2 = \frac{N}{8\pi^2(\Delta T/T)^2\overline{A}^2 L_0}\ \frac{1}{(\mathrm{E_s}/N_0)^2}, \tag{21}$$

$$\sigma_{SN}^2 = \frac{1-\overline{B}}{4\pi^2(\Delta T/T)^2\overline{A}^2 L_0}\ \frac{1}{\mathrm{E_s}/N_0}, \tag{22}$$

$$\sigma_{SS}^2 = \frac{1}{8\pi^2(\Delta T/T)^2\overline{A}^2 L_0}\ \sum_{r=-(L+2)}^{L+2}\left(1-\frac{|r|}{L_0}\right)C(r), \tag{23}$$

where the following notations have been used:

- $\overline{B}$ is defined as

$$\overline{B} = \frac{1}{N}\sum_{k=0}^{N-1} B(kT_s + t_0), \tag{24}$$

where $B(t)$ is the expectation of $\exp\{j[\psi(t)-\psi(t-2\Delta T)\}$ and is obtained from (9) by replacing $a(t)$ with $b(t)=q(t)-q(t-2\Delta T)$.

- $C(r)$ is given by

$$C(r) = \frac{1}{N^2}\sum_{k=0}^{N-1}\sum_{n=0}^{N-1}\left[F^-(kT_s+t_0; nT_s+rT+t_0) - F^+(kT_s+t_0; nT_s+rT+t_0)\right] \tag{25}$$

with

$$F^{\pm}(t_1;t_2) = \prod_i\left[\frac{1}{M}\times\frac{\sin\left\{2\pi hM\left[a(t_1-iT)\pm a(t_2-iT)\right]\right\}}{\sin\left\{2\pi h\left[a(t_1-iT)\pm a(t_2-iT)\right]\right\}}\right]. \tag{26}$$

It is worth noting that the dependence of $\overline{A}$, $\overline{B}$, $C(r)$ and, ultimately, of σ^2 on the sampling phase t_0 is only apparent. As the sampling rate is sufficiently high to avoid aliasing, all the information on the signal (and, therefore, on its parameters $\overline{A}$, $\overline{B}$ and $C(r)$) is conveyed by the samples $x(k)$, whatever the value of t_0. This is confirmed by numerical calculations which show that the above quantities do not change with t_0.

It is seen that σ_{NN}^2 and σ_{SN}^2 are inversely proportional to L_0. This is also true for σ_{SS}^2 when L_0>>1. In these conditions doubling L_0 amounts to reducing the overall estimation errors by 3 dB. It is also clear from the above formulas that σ_{NN}^2 is the dominant term at low SNR, while σ_{SS}^2 sets the floor of the error variance when SNR increases.

5. Simulation Results

Simulations have been run to check the above results and assess the estimator performance with various modulation formats. The brick-wall LPF is approximated with an eight-order Butterworth FIR filter with a 3-dB bandwidth equal to either $2/T$ or $3/T$. Correspondingly, the oversampling factor is either N=4 or N=6.

Figure 4 shows $E\{\hat{\nu}\}$ versus ν for MSK. Here the filter bandwidth equals $2/T$, the delay is $T/2$ and L_0=200. As expected, $E\{\hat{\nu}\}$ approaches zero at the boundaries $\pm 1/T$.

Figure 5 illustrates analogous results for four-level modulation. The parameter L_0 is as before while the delay equals $T/3$ and the filter bandwidth is increased to $3/T$, to take account of the broader signal bandwidth.

Figures 6-7 show σ^2 versus E_b/N_0 for MSK and GMSK ($E_b=E_s/\log_2 M$ is the signal energy per bit of information).

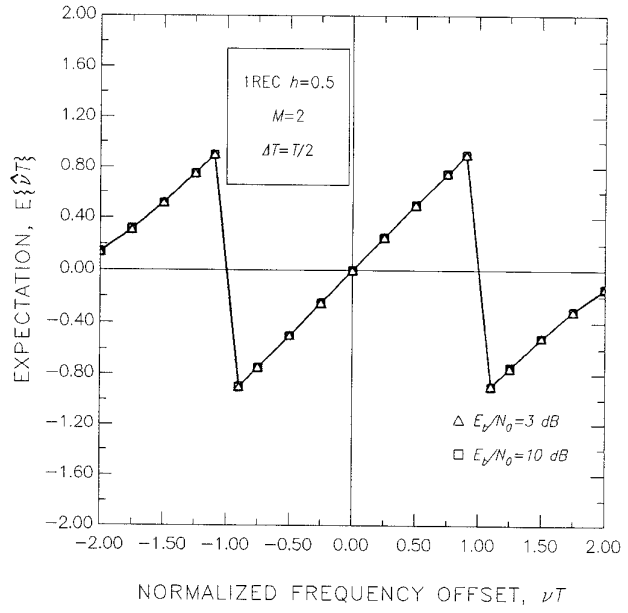

Fig. 4. Expectation $E\{\hat{\nu}\}$ versus ν with MSK. $B_{LPF}=2/T$ and $L_0=200$.

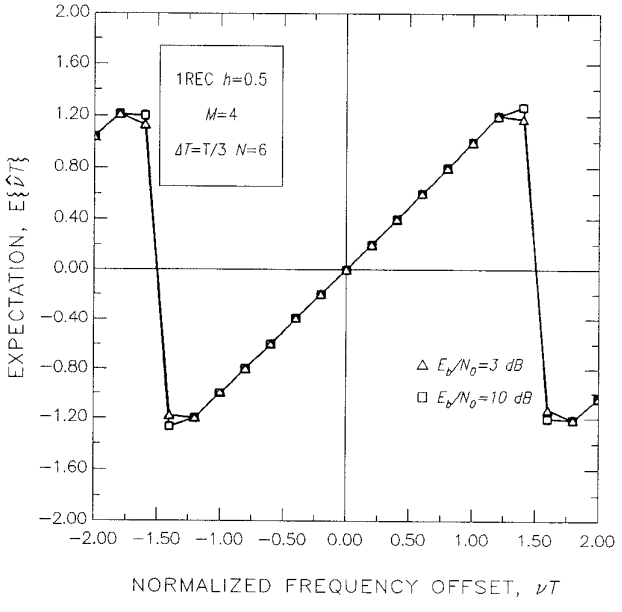

Fig. 5. Expectation $E\{\hat{\nu}\}$ versus ν with $M=4$. $B_{LPF}=3/T$ and $L_0=200$.

In both cases the LPF bandwidth equals $2/T$, and the frequency offset is set to zero. Good agreement is observed between theory and simulations. Indications about the optimum delay are mixed. For example, with MSK, $\Delta T=T/4$ seems better at high SNR but the balance is reversed at low SNR. Similar results have been observed with other *binary* modulations. With quaternary and octal schemes, instead, the value $\Delta T=T/4$ appears definitely the best.

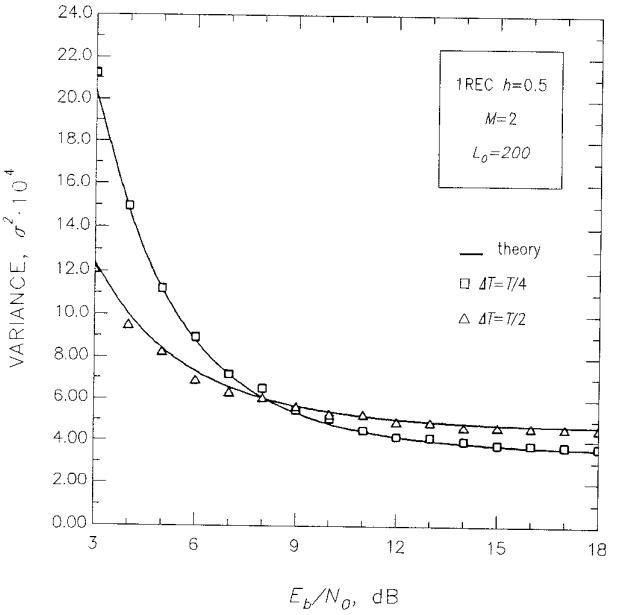

Fig. 6. Error variance versus E_b/N_0. $B_{LPF}=2/T$.

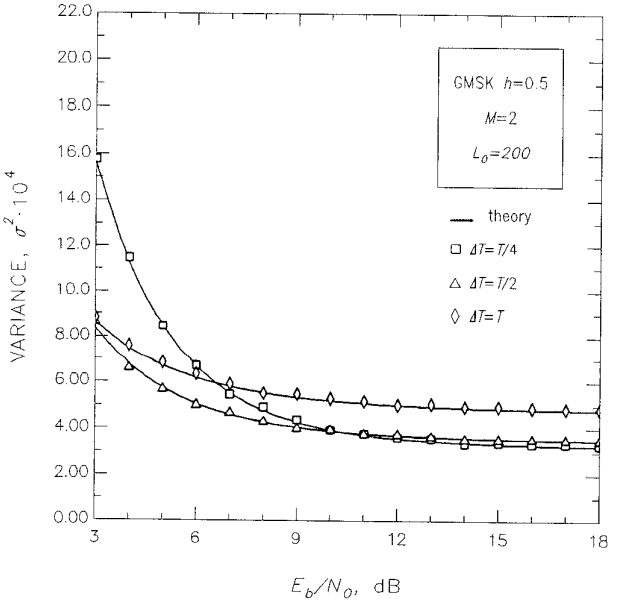

Fig. 7. Error variance versus E_b/N_0 with GMSK. $B_{LPF}=2/T$.

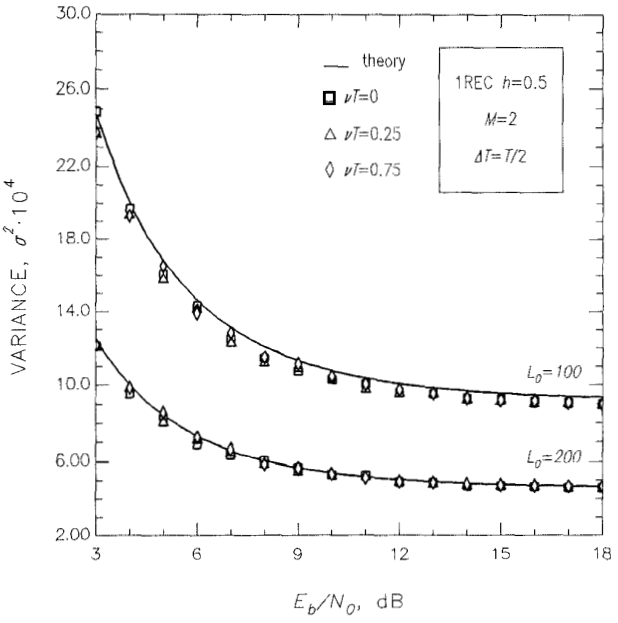

Fig. 8. Error variance versus E_b/N_0 for a few values.$B_{LPF}=2/T$.

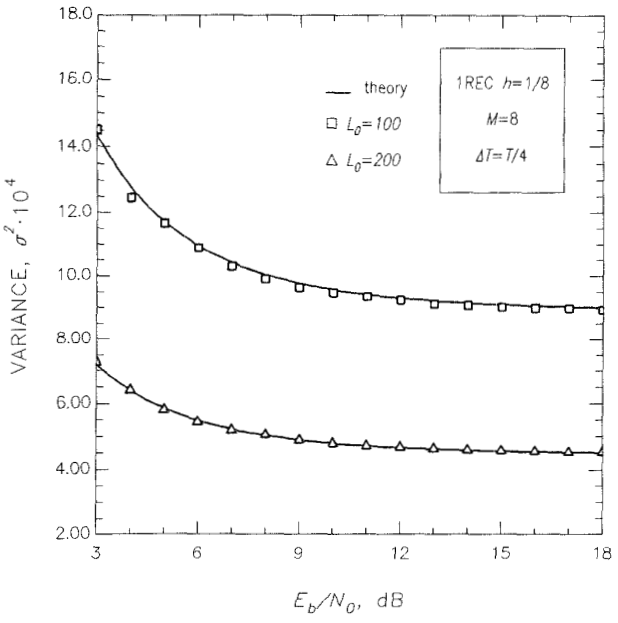

Fig. 9. Error variance versus E_b/N_0 with octal modulation. $B_{LPF}=2/T$.

Figure 8 indicates that previous results are not affected by a non-zero frequency offset, as long as ν remains at a distance from the boundaries of the stimation range.

Figure 9 illustrates the error variance for octal modulation with 1REC pulses and h=1/8.

6. Conclusions

A feedforward frequency estimator for M-ary CPM signals has been analyzed. This scheme does not need clock timing nor data information and is suitable for a digital implementation. Key estimation parameters have been computed analytically and checked by simulation. The estimation range of the estimation algorithm is much larger than in the schemes in [1]-[2]. Errors, on the other hand, are larger. This seems to confirm the unproven observation that accuracy and estimation range are conflicting requirements in carrier frequency recovery.

References

[1] M.Luise and R.Reggiannini, "An Efficient Carrier Frequency Recovery Scheme for GMSK Receivers", Conf. Rec. GLOBECOM'92, CTMC, pp. 36-40, Orlando, FL

[2] R.Melhan, Y-E.Chen and H.Meyr, "A Fully Digital Feedforward MSK Demodulator with Joint Frequency Offset and Symbol Timing Estimation for Burst Mode Mobile Radio", IEEE Trans. Veh. Tech., vol. 42, pp.434-443, Nov. 1993.

[3] A.N.D'Andrea, A.Ginesi and U.Mengali, "Frequency Detectors for CPM Signals", accepted for publication in IEEE Trans. Commun.

[4] F.Classen and H.Meyr, "Two Frequency Estimation Schemes Operating Independently of Timing Information", Conf. Rec. GLOBECOM'93, pp. 1996-2000, Houston, TX.